

PIAT: Parameter Interpolation based Adversarial Training for Image Classification

Kun He*, Xin Liu*, Yichen Yang*

School of Computer Science and Technology,
Huazhong University of Science and Technology, Wuhan, China
{brooklet60, liuxin-jhl, yangyc}@hust.edu.cn

Zhou Qin, Weigao Wen, Hui Xue
Alibaba Group, China

{qinzhou.qinzhou, weigao.wwg, hui.xueh}@alibaba-inc.com

John E. Hopcroft

Department of Computer Science, Cornell University, Ithaca, NY, USA
jeh@cs.cornell.edu

Abstract

Adversarial training has been demonstrated to be the most effective approach to defend against adversarial attacks. However, existing adversarial training methods show apparent oscillations and overfitting issue in the training process, degrading the defense efficacy. In this work, we propose a novel framework, termed Parameter Interpolation based Adversarial Training (PIAT), that makes full use of the historical information during training. Specifically, at the end of each epoch, PIAT tunes the model parameters as the interpolation of the parameters of the previous and current epochs. Besides, we suggest to use the Normalized Mean Square Error (NMSE) to further improve the robustness by aligning the clean and adversarial examples. Compared with other regularization methods, NMSE focuses more on the relative magnitude of the logits rather than the absolute magnitude. Extensive experiments on several benchmark datasets and various networks show that our method could prominently improve the model robustness and reduce the generalization error. Moreover, our framework is general and could further boost the robust accuracy when combined with other adversarial training methods.

1. Introduction

Deep neural networks (DNNs) have been widely used in various tasks of computer vision [8] and natural language processing [12]. However, even the model perfor-

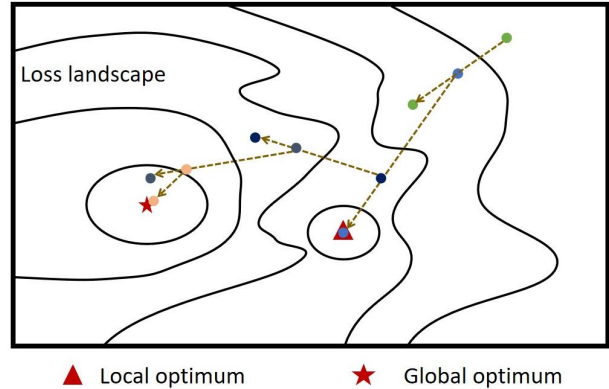


Figure 1: Illustration of the parameter update for the proposed method. The start and end points of each epoch are in colored dots.

mance surpasses humans in some tasks, they are known to be vulnerable to adversarial examples by injecting malicious and imperceptible perturbations to clean inputs that can cause the model to misclassify inputs with the high confidence [23, 7, 16, 3, 1, 9, 26, 17]. Since DNNs are applied in many safety systems, it is of great importance to make them more reliable and robust.

To improve the model’s robustness against adversarial attacks, Adversarial Training (AT) is known to be the most effective approach to defend against adversarial attacks, which generates adversarial examples during the training and incorporates them into the training. However, the training

*The first three authors contributed equally. Correspondence to Kun He.

process of AT has apparent oscillations in the early stage and overfitting issues in the later stage. In the early stage, the model parameters are updated rapidly with a large learning rate, thus the adversarial examples generated at each epoch are pretty different, leading to the oscillation on robust accuracy. In the later stage, many works [27, 20, 6] and our experiments have shown that the overfitting issue occurs in the later stage of AT, that is, the training accuracy continues to increase but the robust accuracy on the testing data begins to decline.

To solve the oscillation issue in the early stage of AT and the overfitting issue in the later stage, we propose a Parameter Interpolation based Adversarial Training (PIAT) framework. As illustrated in Figure 1, at the end of each epoch of the training, we tune the model parameters as the interpolation of the model parameters of the previous and current epochs. In the early stage of AT, the adversarial examples generated at each epoch is significantly different, and the model’s decision boundary changes dramatically. In contrast, PIAT tunes the model parameters with the previous epoch and makes the change of the decision boundary more moderate, helping to eliminate the oscillation. In the later stage, PIAT considers the previous boundary, preventing the decision boundary from becoming too complex and alleviating the overfitting issue. As the training continues and the model parameters become more valuable, PIAT gradually increases the weight of the previous parameters when tuning the current parameters.

On the other hand, we observe that some works, such as TRADES [29] and MART [24], assume that the data distribution between clean and adversarial examples are virtually indistinguishable. To improve the performance of AT, they propose regularization terms to force the model output for clean and adversarial examples to be as similar as possible. However, the data distribution between clean and adversarial examples is quite different, and simply forcing the output to be close is too demanding. We suggest that AT should pay more attention to aligning the relative magnitude rather than the absolute magnitude of logits between the clean and adversarial examples. Hence, we propose a new metric called Normalized Mean Square Error (NMSE) to better align the clean and adversarial examples. NMSE pays more attention to the relative magnitude of the output of clean examples and adversarial examples rather than the absolute magnitude, thus learning the common information of different distributed data.

We incorporate the Normalized Mean Square Error (NMSE) as the regularization into the proposed PIAT framework. Extensive experiments on CIFAR10, CIFAR100, and SVHN datasets show that our method performs better and effectively improves the adversarial robustness of the model against white-box and black-box attacks. In addition, our PIAT framework is general and other adversarial training

methods can be incorporated into our framework to achieve better robustness and performance.

Our main contributions are summarized as follows:

- To solve the oscillation issue in the early stage of AT and the overfitting issue in the later stage, we propose the PIAT framework that interpolates the model parameters of the previous and current epochs to consider the historical information during the training.
- We propose to use the NMSE loss as a new regularization term to better align the logits of clean and adversarial examples. NMSE pays more attention to the relative magnitude of the output of clean examples and adversarial examples rather than the absolute magnitude.
- The robust accuracy of our method is stable, indicating that PIAT alleviates the oscillation and overfitting issues during the AT process. Extensive experiments on three standard datasets and two networks show that PIAT combined with NMSE offers excellent robustness without incurring additional cost.

2. Related Work

2.1. Adversarial Training

Adversarial training (AT) [16] has been demonstrated to be the most effective defensive methods against adversarial attacks, which generates a locally most adversarial perturbed point for each clean example and trains the model to classify them correctly.

Given an image classification task, the training dataset $D = \{(\mathbf{x}_i, y_i)\}_{i=1}^n$ consists of n clean examples with c classes, where $\mathbf{x}_i \in \mathbb{R}^d$ represents a clean example with the ground-truth label $y_i \in \{1, 2, \dots, c\}$. The adversarial training optimization problem can be formulated as the following min-max problem:

$$\min_{\theta} \sum_i \max_{\mathbf{x}'_i \in \mathbf{S}(\mathbf{x}_i, \epsilon)} \mathcal{L}(f_{\theta}(\mathbf{x}'_i, y_i)), \quad (1)$$

where $f_{\theta}(\cdot) : \mathbb{R}^d \rightarrow \mathbb{R}^c$ is the DNN classifier with parameter θ . $\mathcal{L}(\cdot, \cdot)$ represents the cross entropy loss and $\mathbf{S}(\mathbf{x}_i, \epsilon) = \{\|\mathbf{x}'_i - \mathbf{x}_i\|_p \leq \epsilon\}$ represents an ϵ -ball of a benign data point \mathbf{x}_i . \mathbf{x}'_i denotes the adversarial example generated from \mathbf{x}_i .

To solve the inner maximization problem, the adversarial example \mathbf{x}'_i is often crafted by the Projected Gradient Decent (PGD) attack [16], which can be formulated by:

$$\mathbf{x}_i^{t+1} = \prod_{\mathbf{S}(\mathbf{x}_i)} (\mathbf{x}_i^t + \alpha \cdot \text{sign}(\nabla_{\mathbf{x}_i^t} \mathcal{L}(f_{\theta}(\mathbf{x}_i^t), y_i))). \quad (2)$$

Here \mathbf{x}_i^t denotes the adversarial example at the t^{th} step, $\prod(\cdot)$ is the projection operator and α is the step size.

TRADES [29] is another typical AT proposed to achieve a better balance between accuracy on clean examples and robustness on adversarial examples:

$$\min_{\theta} \sum_i \{CE(f_{\theta}(\mathbf{x}_i), y_i) + \beta \cdot \max_{\mathbf{x}'_i \in \mathcal{S}(\mathbf{x}_i, \epsilon)} KL(f_{\theta}(\mathbf{x}_i) || f_{\theta}(\mathbf{x}'_i))\}, \quad (3)$$

where $CE(\cdot, \cdot)$ is the cross entropy loss that maximize the accuracy of clean examples. $KL(\cdot || \cdot)$ is the Kullback-Leibler divergence that measures the distance of output between clean and adversarial examples and β controls the tradeoff between accuracy and robustness.

Since the inception of TRADES, subsequent efforts have been devoted to achieve better performance. MART [24] explicitly differentiates the misclassified and correctly classified examples during the training. STAT [15] takes both adversarial examples and collaborative examples into account for regularizing the loss landscape. FreeAT [21] uses each epoch of PGD adversarial examples and updates the model with the gradient. Among the adversarial data that are confidently misclassified, rather than employing the most adversarial data that maximize the loss, FAT [30] searches for the least adversarial data that minimize the loss. LAS-AT [10] learns to automatically produce attack strategies to improve the model robustness. SCORE [19] facilitates the reconciliation between robustness and accuracy, while still handling the worst-case uncertainty via robust optimization.

2.2. Decision Boundary and Overfitting

Dong *et al.* [6] have found that the decision boundaries for adversarial training are more complex than those for standard training, thus making the training more difficult. LBGAT [4] constrains logits from the robust model that takes adversarial examples as input and makes it similar to those from the clean model fed with the corresponding natural data to better fine-tune the decision boundaries.

Moreover, overfitting issue widely exists during the course of adversarial training [20]. GAIRAT [31] adjusts the weights based on the difficulty of attacking a benign data point. AWP [25] explicitly regularizes the flatness of the weight loss landscape, forming a double-perturbation mechanism in the adversarial training framework that adversarially perturbs both inputs and weights. RLFAT [22] learns robust local features by adversarial training on the random block shuffle transformed adversarial examples, and then transfers the robust local features into the training of normal adversarial examples. MLCAT [27] learns large-loss data as usual, and adopts additional measures to increase the loss of small-loss data to hinder data fitting when the data become easy to learn.

Nevertheless, the classification accuracy of adversarial training on clean and adversarial examples still has room

for improvement. After each epoch of parameter updates on the model, different adversarial examples are generated. Compared with clean examples, adversarial examples are much more diverse, making it hard for the training to learn from the data when the network capacity is rather limited. In this work, we observe that previous works did not fully utilize the historical information during training, thus we proposed to utilize historical information to boost the model’s robustness.

3. Motivation

This section further analyzes the oscillations in the early stage and the overfitting issue in the later stage of the AT process. Based on our observations, we propose to fully utilize the historical training information by parameter interpolation at the end of each epoch. We also discuss aligning clean and adversarial examples in AT and suggest focusing more on the relative magnitude of the output logits rather than the absolute magnitude.

3.1. Analysis on the Robust Accuracy

Figure 2 illustrates the test accuracy on clean and adversarial examples of several popular AT methods during training, including PGD-AT [16], ALP [11], FAT [30], TRADES [29], MART [24] and GAIRAT [31]. As illustrated in Figure 2 (b), over all these AT methods except our method (PIAT + NMSE), we can observe that in the early stage, there are apparent oscillations in terms of robust accuracy, and in the later stage, the adversarial robustness all declines as the model overfits adversarial examples.

In the early stage, the model has not learned to fit the data yet and model parameters are updated with a large learning rate, leading to rapid changes on the decision boundary. Subsequently, the adversarial examples generated by the PGD attack for adversarial training vary significantly at each epoch. Thus, it is hard for the models to learn the features and have good generalization from the changing data, making the robust accuracy unstable. If the change on decision boundary is more moderate, then the difference of adversarial examples generated between two adjacent epochs will be smaller. A straightforward solution is to reduce the learning rate. However, a low learning rate will decelerate the convergence of AT. Worse still, the oscillation may disappear with a low learning rate, but the overfitting issue occurs.

In the later stage, as the learning rate of most AT methods is reduced significantly, the decision boundary will become overly complex when the model struggles to well fit the adversarial examples crafted during training. As a result, the learned model is not robust enough to well handle unseen adversarial examples, leading to the overfitting issue.

We observe that existing AT methods ignore the historical information in the training process, which would be useful to stabilize the training and alleviate overfitting. To this end, we

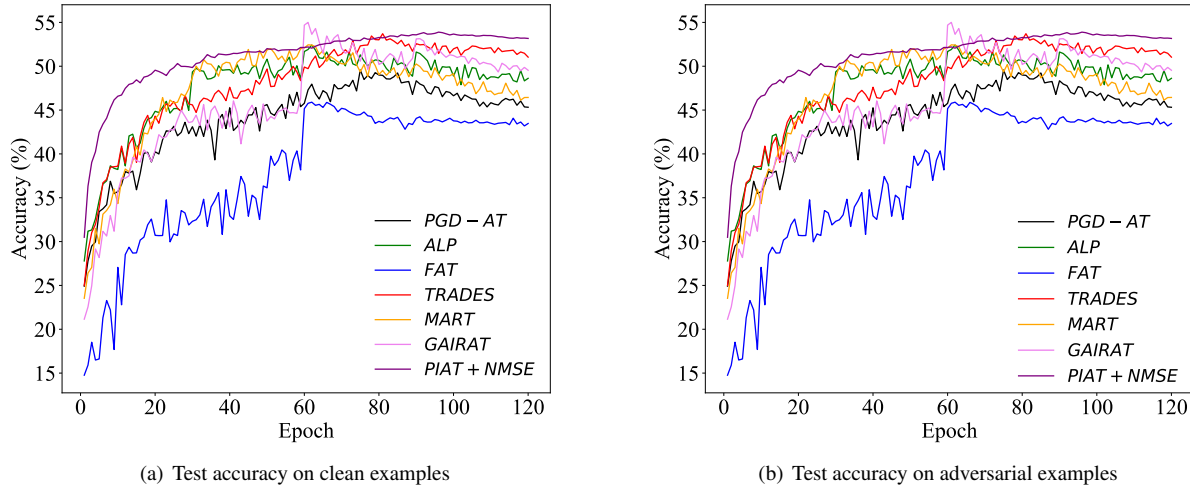


Figure 2: Test accuracy on clean and adversarial examples of ResNet18 trained by various AT methods on CIFAR10.

propose to utilize the model parameters of previous epoch to fine-tune the current parameters at the end of each epoch. Such an approach allows us to leverage historical information and improve the the robust generalization capability. In the early stage, considering parameters of the previous epoch will result in a more gradual update on the model parameters, helping to ensure a smoother and more stable training. In the later stage, mixing parameters of the previous epoch could smooth the decision boundary and prevent the model from overfitting.

3.2. Analysis on the AT Regularization

Combining regularization with the loss of standard AT is one of the most effective ways to alleviate the overfitting issue and improve the model robustness. For instance, the Kullback-Leibler (KL) divergence between the classification probabilities of clean and adversarial examples is often used for regularization [29]. Minimizing the KL divergence aligns the prediction of clean and adversarial examples and encourages the output to be smooth.

However, adversarial examples contain malicious noise that substantially deviates from the data distribution of clean examples. We argue that it is too demanding to force the absolute magnitude of output predictions to remain the same on the two types of examples. Moreover, the KL divergence compares the classification probabilities obtained through the softmax operation on logits. This operation tends to amplify the probability of the correct class while reducing that of other classes. AT can not fully learn the information from adversarial examples by focusing too much on the output probability of the correct class but neglecting probabilities of other classes.

Therefore, it is more reasonable that the output logits for clean examples and adversarial examples are roughly similar but not identical. Rather than considering the absolute magnitude of the output logits, we should pay more attention to the relative magnitude between clean and adversarial examples.

4. Methodology

In this section, we introduce the realization of the PIAT framework. We also describe how to combine with our proposed Normalized Mean Square Error (NMSE).

4.1. The PIAT Framework

To fully utilize the historical information during training, at the end of each epoch, PIAT tunes the model parameters as the interpolation of parameters of the previous and current epochs, which can be formalized as:

$$\theta'_t = \lambda \cdot \theta'_{t-1} + (1 - \lambda) \cdot \theta_t, \quad 0 \leq \lambda \leq 1, \quad (4)$$

where θ'_{t-1} is the model parameters of the previous epoch after interpolation, and θ_t is current parameters before interpolation at the end of the training epoch. Then, before starting the next epoch, we tune the parameters to θ'_t . The hyper-parameter λ controls the trade-off between previous and current parameters.

The value of λ is critical to PIAT. In the early stage of AT, the model has not yet fit the training data well enough. Thus, the model is not robust enough against adversarial attacks, and its parameters are not very informative. If λ is too large, the model mainly relies on previous parameters and learns

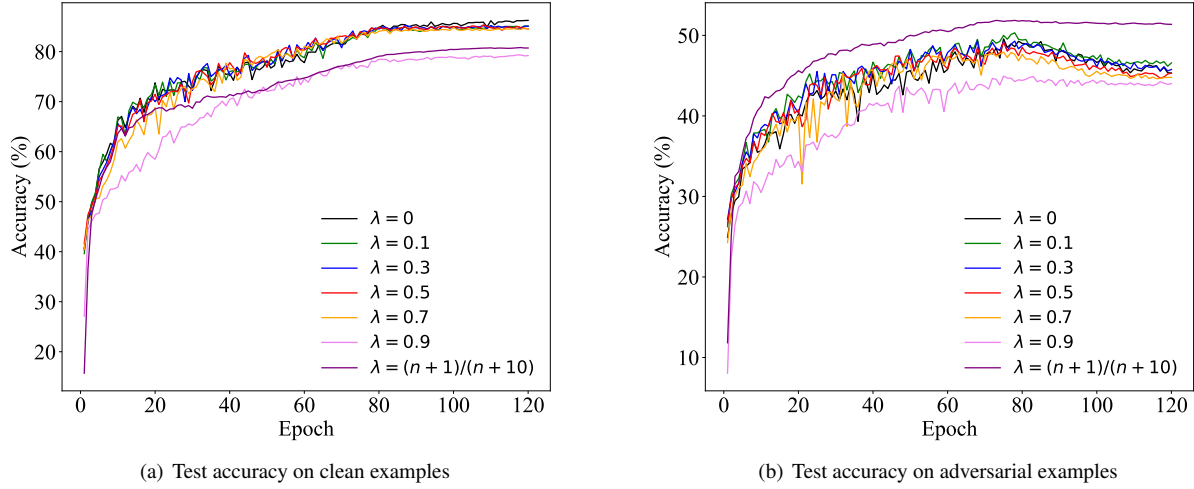


Figure 3: The accuracy on clean and adversarial examples of ResNet18 models trained by PIAT with different λ on the CIFAR10 dataset. n denotes the current number of training epochs.

Algorithm 1 The PIAT Framework

Input: Initial model parameters θ_0 , perturbation size ϵ , number of adversarial attack steps K , number of epochs N, N_0 , weight function $g(\cdot)$

Output: θ'_N

Initialize $\theta \leftarrow \theta_0$

for $i = 1$ **to** N_0 **do**

for minibatch $\mathbf{x} \subset \mathbf{X}$ **do**

$loss = \mathcal{L}_{CE}(\mathbf{x}, y)$

update θ_i

end for

end for

$\theta'_0 \leftarrow \theta_{N_0}$

for $i = 1$ **to** N **do**

$\theta_i \leftarrow \theta'_{i-1}$

for minibatch $\mathbf{x} \subset \mathbf{X}$ **do**

$\mathbf{x}_{adv} \leftarrow \mathbf{x}$

for $k = 1$ **to** K **do**

$\mathbf{x}_{adv} \leftarrow \mathbf{x}_{adv} + \epsilon \cdot \text{sign}(\nabla_{\mathbf{x}} \mathcal{L}_{CE}(\mathbf{x}_{adv}, y))$

$\mathbf{x}_{adv} \leftarrow \text{clip}(\mathbf{x}_{adv}, \mathbf{x} - \epsilon, \mathbf{x} + \epsilon)$

end for

$loss = \mathcal{L}(\mathbf{x}_{adv}, y)$

update θ_i

end for

$\lambda \leftarrow g(i)$

$\theta'_i \leftarrow \lambda \cdot \theta'_{i-1} + (1 - \lambda) \cdot \theta_i$

end for

return θ'_N

the training data in small steps, leading to slow convergence. Therefore, λ should be small in the early stage.

As the training continues, the model starts to learn enough information from the adversarial examples and attains adversarial robustness. In the later stage, the model has learned enough information and gained good robustness. λ should be close to 1, otherwise the model tends to discard useful information learned over the training process and overfit the current adversarial examples.

According to the above analysis, λ should change over the course of training, instead of using a fixed value. The value of λ should be small in the early stage of training and gradually increase along with the training, which not only ensures the convergence speed but also alleviates the overfitting issue in AT. In this paper, we set λ as follows:

$$\lambda = g(n) = \frac{n+1}{n+c}, \quad c \geq 1, \quad (5)$$

where n denotes the current number of training epochs. c is a hyper-parameter and we set $c = 10$ in this work. The accuracy curves of different λ values are as shown in Figure 3. We will verify that a dynamic λ that varies with the number of training epochs has better robustness against a fixed value in Section 5.4.

Algorithm 1 concludes the overall framework. Since PIAT does not restrict the type of loss function in the framework, it is flexible and can be combined with various adversarial training methods such as TRADES [29], MART [24] and GAIRAT [31].

Table 1: The accuracy (%) of our method and AT baselines under various adversarial attacks on CIFAR10, CIFAR100 and SVHN datasets with ResNet18 model.

DATASET	METHOD	NAT	PGD ²⁰	PGD ¹⁰⁰	MIM	CW	AA
CIFAR10	PGD-AT	84.28	50.29	50.12	51.21	49.31	46.33
	TRADES	82.39	53.60	53.65	54.55	50.90	48.04
	MART	81.91	53.70	53.70	54.95	49.35	47.45
	GAIRAT	81.69	55.84	55.90	56.62	45.50	40.85
	PIAT	79.08	51.81	51.74	52.63	49.32	47.08
	PIAT +NMSE	80.76	53.54	53.59	54.51	51.72	48.80
CIFAR100	PGD-AT	58.48	28.36	28.33	29.30	27.06	23.85
	TRADES	57.98	29.90	29.88	29.55	26.14	24.72
	MART	55.26	30.10	30.16	30.51	26.00	23.77
	GAIRAT	50.26	23.33	23.35	23.90	21.55	19.26
	PIAT	58.84	29.11	29.14	29.97	27.89	24.15
	PIAT +NMSE	54.34	31.11	30.99	31.42	28.45	25.79
SVHN	PGD-AT	93.85	59.01	58.92	59.93	48.66	43.02
	TRADES	90.88	59.50	59.43	60.52	52.76	46.59
	MART	88.73	59.45	59.42	59.83	60.19	44.65
	GAIRAT	90.50	54.14	54.09	55.88	50.71	44.57
	PIAT	92.15	59.53	59.61	61.32	55.54	50.93
	PIAT +NMSE	91.70	61.21	61.43	61.97	55.88	51.29

4.2. The NMSE Regularization

According to the discussion in Section 3, instead of aligning the clean and adversarial examples by classification probabilities, we utilize the output logits normalized with l_2 -norm.

We align the clean and adversarial examples by minimizing the mean square error between their normalized output logits. Besides, we set $(1 - p_{clean})$ as the weight for different adversarial examples so that the model will pay more attention to the clean examples which are vulnerable. We formulate the Normalized Mean Square Error (NMSE) regularization as follows:

$$\mathcal{L}_{NMSE} = (1 - p_{clean}) \cdot \left\| \frac{f_{\theta}(\mathbf{x})}{\|f_{\theta}(\mathbf{x})\|_2} - \frac{f_{\theta}(\mathbf{x}')}{\|f_{\theta}(\mathbf{x}')\|_2} \right\|_2^2, \quad (6)$$

where \mathbf{x}' is the adversarial example, $f_{\theta}(\mathbf{x})$ is the output logits of the model, and $\|\cdot\|_2$ denotes l_2 -norm of vector.

In summary, the overall loss function in PIAT framework with NMSE is as follows:

$$\mathcal{L} = \mathcal{L}_{CE} + \mu \cdot \mathcal{L}_{NMSE}, \quad (7)$$

where μ is a hyper-parameter to trade off the cross-entropy loss \mathcal{L}_{CE} on adversarial examples and the NMSE regularization term \mathcal{L}_{NMSE} .

5. Experiments

In this section, we conduct experiments on several benchmark datasets to evaluate the defense efficacy of our PIAT framework and NMSE regularization. We also verify that PIAT could boost the model robustness when combined with various AT methods.

5.1. Experimental Setup

Datasets and Models We conduct experiments on three benchmark datasets including CIFAR10 [13], CIFAR100 [13], and SVHN [18]. All images are normalized into $[0, 1]$. We evaluate on two models, ResNet18 [8] and WRN-32-10 [28], to verify the efficacy of our method.

Evaluation Details We compare the PIAT combined with NMSE regularization with the following AT baselines: TRADES [29], MART [24], and GAIRAT [31]. To thoroughly evaluate the defense efficacy of our method and the baselines, we adopt various adversarial attacks including PGD [16], MIM [5], CW [2], and AA [3].

Training Details For all the experiments, we train ResNet18 (WRN-32-20) using SGD with 0.9 momentum for 120 (180) epochs. The weight decay is 3.5×10^{-3} for ResNet18 and 7×10^{-4} for WRN-32-10 on three datasets. The initial learning rate for ResNet18 (WRN-32-10) is 0.01 (0.1) till epoch 60 (90) and then linearly decays to 0.001 (0.01), 0.0001 (0.001) at epoch 90 (135) and 120 (180). To address the cold boot problem of training, we perform stan-

Table 2: The accuracy (%) of our method and AT baselines under adversarial attacks on CIFAR10 and CIFAR100 datasets with WRN-32-10 model.

DATASET	METHOD	NAT	PGD ²⁰	AA
CIFAR10	PGD-AT	86.87	48.77	47.78
	TRADES	82.13	55.14	50.38
	PIAT	85.56	52.80	48.35
	PIAT +TRADES	82.08	58.93	53.73
	PIAT +NMSE	85.04	58.04	53.83
CIFAR100	PGD-AT	59.30	28.13	23.99
	TRADES	57.99	31.97	26.76
	PIAT	60.09	34.46	29.47
	PIAT +TRADES	59.78	34.52	29.25
	PIAT +NMSE	61.04	35.15	30.07

Table 3: The accuracy (%) of AT methods with or without NMSE regularization under adversarial attacks on CIFAR10 and CIFAR100 dataset with ResNet18 model.

DATASET	METHOD	NAT	PGD ²⁰	AA
CIFAR10	PGD-AT	84.28	50.29	46.33
	PGD-AT+NMSE	84.77	51.56	46.60
	PIAT	79.08	51.81	47.08
	PIAT +NMSE	80.76	53.55	48.70
CIFAR100	PGD-AT	58.48	28.36	23.85
	PGD-AT+NMSE	58.88	29.55	24.82
	PIAT	58.84	29.11	24.15
	PIAT +NMSE	54.34	31.11	25.79

ard training on the clean data for the first 10 epochs, and then perform adversarial training. For crafting adversarial examples, the maximum perturbation of each pixel is $\epsilon = \frac{8}{255}$ with the PGD step size $\kappa = \frac{2}{255}$ and step number of 10. For the baseline of TRADES, we adopt $\beta = 6$ for the best robustness.

5.2. Evaluation on Defense Efficacy

We compare the defense efficacy of our method with four AT baselines including PGD-AT, TRADES, MART and GAIRAT. Table 1 reports the accuracy of ResNet18 model trained with our method or the defense baselines under various adversarial attacks on three datasets.

As shown in Table 1, our method (PIAT + NMSE) exhibits the best performance except for the PGD and MIM attack on CIFAR10 dataset. Under the AA attack, our method achieves 48.80%, 25.79% and 51.29% accuracy on CIFAR10, CIFAR100 and SVHN datasets. Compared to the best results of defense baselines, we gain an improvement of

0.76%, 1.07% and 5.50% on the three datasets, respectively, indicating the great superiority of our method.

We do further evaluation on the WRN-32-10 model, which is much larger than ResNet18, and compare our method with PGD-AT and TRADES. The results are reported in Table 2. Similar to the results on ResNet18, our method achieves the dominant robustness with a clear margin, especially on CIFAR10 dataset.

5.3. Ablation Study

PIAT Framework Since PIAT is a general framework, we incorporate other AT methods into PIAT to demonstrate its defense efficacy. Figure 4 illustrates the accuracy of PIAT framework combined with TRADES, MART, and GAIRAT, respectively, under the AA attack on the three datasets.

As shown in Figure 4, over all the three datasets, PIAT boosts the robustness of various AT methods against the AA attack. The results demonstrate that we can easily incorporate other AT methods into our PIAT framework without incurring any additional cost to achieve better robustness and performance.

We also do ablation study on the WRN-32-10 model and report the results in Table 2. Specifically, PIAT framework significantly boosts the robust accuracy of TRADES, gaining absolute improvement of 3.35% and 2.49% on CIFAR10 and CIFAR100 under the AA attack, respectively. Our framework leads to higher robust accuracy when combined with other AT methods on two models, indicating that PIAT has good flexibility and generalization.

NMSE Regularization To evaluate the effectiveness of our proposed NMSE regularization, we observe the performance of PGD-AT and PIAT with or without NMSE regularization. Table 3 reports the accuracy of ResNet18 models against PGD and AA attack on the CIFAR10 and CIFAR100 datasets.

As shown in Table 3, both PGD-AT and PIAT achieve better robustness with NMSE regularization than that without NMSE. For instance, the accuracy of PGD-AT against AA attack gains absolutely 0.37% and 1.62% on CIFAR10 and CIFAR100, respectively. It indicates that the NMSE regularization greatly helps the model learn the features of adversarial examples.

5.4. Further Analysis

We continue to analyze the sensitivity of hyper-parameters in our method. Besides, we draw a 3D visual landscape of loss function to further compare our method and PGD-AT.

Hyper-parameter Analysis The hyper-parameter λ in Eq. 4 is used to control the trade-off between previous and current parameters for PIAT. In Section 3, we intuitively suggest that λ should change over the course of training, instead of using a fixed value. To verify this point, we

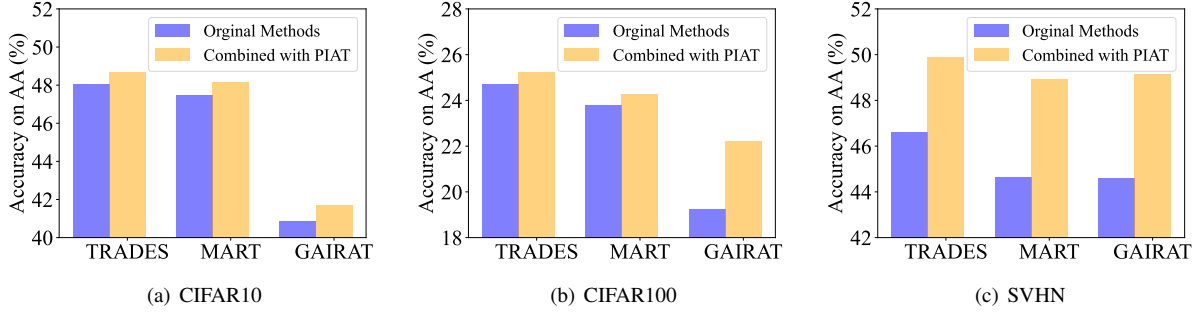


Figure 4: The accuracy of the PIAT framework combined with various AT methods under the AA attack on CIFAR10, CIFAR100, and SVHN datasets with ResNet18 model.

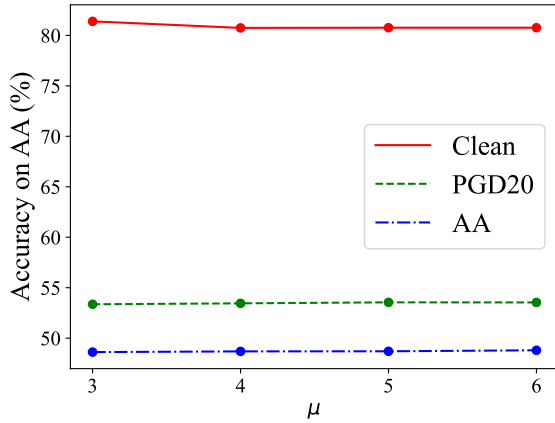


Figure 5: The clean and robust accuracies of different hyper-parameters of NMSE loss combined with PIAT framework on CIFAR10. Different lines represent the defensive efficacy of clean and adversarial examples.

compare the accuracy of PIAT combined with NMSE using fixed $\lambda = 0, 0.1, 0.3, 0.5, 0.7, 0.9$ and our variable λ as in Eq. 5. Figure 3 illustrates the results on the CIFAR10 dataset. It is obvious that the variable strategy of λ is vital to alleviate the oscillations in the early stage and the overfitting issue in the later stage of the AT process.

The hyper-parameter μ in Eq. 7 is used to trade off the cross-entropy loss on adversarial examples and the NMSE regularization term. We study the accuracy of PIAT combined with NMSE using different μ . Figure 5 illustrates the results on the CIFAR10 dataset when we take $\mu = 3, 4, 5, 6$. It indicates that the defensive efficacy of our method is not sensitive to μ . Similar observations can be obtained on the CIFAR-100 dataset. Therefore, we set $\mu = 5$ in our experiments for an appropriate trade-off between the accuracy on clean and adversarial examples.

Loss Landscape To comprehensively evaluate the ef-

ficacy of our framework, we refer to the method proposed by Li *et al.* [14] and compare the model obtained by PIAT framework and PGD-AT in 3D. Let \mathbf{u} and \mathbf{v} be two random direction vectors sampled from the Gaussian distribution. We plot the loss landscape around θ of the following equation when inputting the same data:

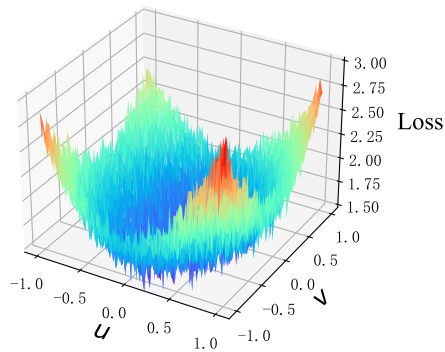
$$\mathcal{L}(\theta; \mathbf{u}; \mathbf{v}) = \mathcal{L} \left(\theta + m_1 \frac{\mathbf{u}}{\|\mathbf{u}\|} + m_2 \frac{\mathbf{v}}{\|\mathbf{v}\|} \right), \quad (8)$$

where $m_1, m_2 \in [-1, 1]$.

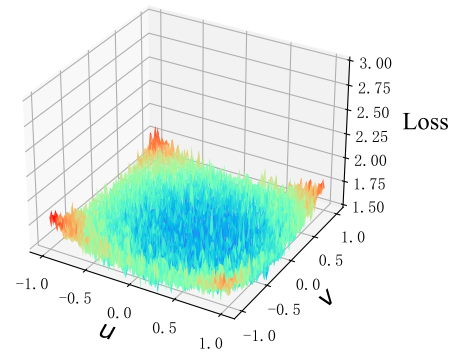
Figure 6 illustrates the shape of the 3D landscape map. We observe that compared with the PGD-AT, the model trained using the PIAT framework exhibits less fluctuation in the loss landscape under the same perturbation. Compared with the PGD-AT, the 3D landscape obtained using the PIAT framework indicates that the model converges to a flatter area and has better robust accuracy.

6. Conclusion

In this work, we propose the PIAT framework to make the decision boundary change more moderately, thus eliminating the oscillation phenomenon in the early stage of AT. Also, in the later stage, PIAT framework considers the decision boundary of previous iteration, preventing the decision boundary from becoming too complex and alleviating the overfitting issue. Moreover, we suggest to use the Normalized Mean Square Error (NMSE) as regularization to align the clean examples and adversarial examples, that focuses more on the relative magnitude of the output logits rather than the absolute magnitude. Extensive experiments verify that our framework can eliminate the oscillation phenomenon and alleviate the overfitting issue of adversarial training. Furthermore, the PIAT combined with NMSE loss could significantly improve the model robustness of adversarial training without extra computational cost. In addition, our framework is flexible and general, and various adversarial



(a) Loss landscape of PGD-AT



(b) Loss landscape of PIAT

Figure 6: Illustration of the loss landscape in three dimensions. Our PIAT framework has flatter loss landscape than PGD-AT.

training methods can be combined into our PIAT framework to further boost their performance.

Our work shows that the historical information of adversarial training process is very useful. We hope our work will inspire more works utilizing historical training information to boost the model robustness.

References

- [1] Anish Athalye, Nicholas Carlini, and David Wagner. Obfuscated gradients give a false sense of security: Circumventing defenses to adversarial examples. In *Proceedings of the 35th International Conference on Machine Learning*, pages 274–283, 2018. 1
- [2] Nicholas Carlini and David Wagner. Towards evaluating the robustness of neural networks. In *2017 IEEE Symposium on Security and Privacy*, pages 39–57, 2017. 6
- [3] Francesco Croce and Matthias Hein. Reliable evaluation of adversarial robustness with an ensemble of diverse parameter-free attacks. In *Proceedings of the 37th International Conference on Machine Learning*, pages 2206–2216, 2020. 1, 6
- [4] Jiequan Cui, Shu Liu, Liwei Wang, and Jiaya Jia. Learnable boundary guided adversarial training. In *Proceedings of the IEEE/CVF International Conference on Computer Vision*, pages 15721–15730, 2021. 3
- [5] Yinpeng Dong, Fangzhou Liao, Tianyu Pang, Hang Su, Jun Zhu, Xiaolin Hu, and Jianguo Li. Boosting adversarial attacks with momentum. In *2018 IEEE Conference on Computer Vision and Pattern Recognition*, pages 9185–9193, 2018. 6
- [6] Yinpeng Dong, Ke Xu, Xiao Yang, Tianyu Pang, Zhijie Deng, Hang Su, and Jun Zhu. Exploring memorization in adversarial training. In *International Conference on Learning Representations*, 2022. 2, 3
- [7] Ian J. Goodfellow, Jonathon Shlens, and Christian Szegedy. Explaining and harnessing adversarial examples. In *International Conference on Learning Representations*, 2015. 1
- [8] Kaiming He, Xiangyu Zhang, Shaoqing Ren, and Jian Sun. Deep residual learning for image recognition. In *2016 IEEE Conference on Computer Vision and Pattern Recognition*, pages 770–778, 2016. 1, 6
- [9] Dan Hendrycks, Kimin Lee, and Mantas Mazeika. Using pre-training can improve model robustness and uncertainty. In *International Conference on Machine Learning*, pages 2712–2721, 2019. 1
- [10] Xiaojun Jia, Yong Zhang, Baoyuan Wu, Ke Ma, Jue Wang, and Xiaochun Cao. Las-at: Adversarial training with learnable attack strategy. In *Proceedings of the IEEE/CVF Conference on Computer Vision and Pattern Recognition*, pages 13398–13408, 2022. 3
- [11] Harini Kannan, Alexey Kurakin, and Ian Goodfellow. Adversarial logit pairing. *arXiv preprint arXiv:1803.06373*, 2018. 3
- [12] Jacob Devlin Ming-Wei Chang Kenton and Lee Kristina Toutanova. Bert: Pre-training of deep bidirectional transformers for language understanding. In *Proceedings of the 2019 Conference of the North American Chapter of the Association for Computational Linguistics: Human Language Technologies*, pages 4171–4186, 2019. 1
- [13] Alex Krizhevsky et al. Learning multiple layers of features from tiny images. 2009. 6
- [14] Hao Li, Zheng Xu, Gavin Taylor, Christoph Studer, and Tom Goldstein. Visualizing the loss landscape of neural nets. In *Advances in Neural Information Processing Systems 31: Annual Conference on Neural Information Processing Systems 2018*, pages 6391–6401, 2018. 8
- [15] Qizhang Li, Yiwen Guo, Wangmeng Zuo, and Hao Chen. Squeeze training for adversarial robustness. In *International Conference on Learning Representations*, 2023. 3

- [16] Aleksander Madry, Aleksandar Makelov, Ludwig Schmidt, Dimitris Tsipras, and Adrian Vladu. Towards deep learning models resistant to adversarial attacks. In *International Conference on Learning Representations*, 2018. 1, 2, 3, 6
- [17] Dongyu Meng and Hao Chen. Magnet: A two-pronged defense against adversarial examples. In *Proceedings of the 2017 ACM SIGSAC Conference on Computer and Communications Security*, pages 135–147, 2017. 1
- [18] Yuval Netzer, Tao Wang, Adam Coates, Alessandro Bissacco, Bo Wu, and Andrew Y Ng. Reading digits in natural images with unsupervised feature learning. In *NIPS Workshop on Deep Learning and Unsupervised Feature Learning*, 2011. 6
- [19] Tianyu Pang, Min Lin, Xiao Yang, Jun Zhu, and Shuicheng Yan. Robustness and accuracy could be reconcilable by (proper) definition. In *International Conference on Machine Learning*, pages 17258–17277, 2022. 3
- [20] Leslie Rice, Eric Wong, and Zico Kolter. Overfitting in adversarially robust deep learning. In *International Conference on Machine Learning*, pages 8093–8104. PMLR, 2020. 2, 3
- [21] Ali Shafahi, Mahyar Najibi, Mohammad Amin Ghiasi, Zheng Xu, John Dickerson, Christoph Studer, Larry S Davis, Gavin Taylor, and Tom Goldstein. Adversarial training for free! *Advances in Neural Information Processing Systems*, 32, 2019. 3
- [22] Chuanbiao Song, Kun He, Jiadong Lin, Liwei Wang, and John E. Hopcroft. Robust local features for improving the generalization of adversarial training. In *8th International Conference on Learning Representations*, 2020. 3
- [23] Christian Szegedy, Wojciech Zaremba, Ilya Sutskever, Joan Bruna, Dumitru Erhan, Ian Goodfellow, and Rob Fergus. Intriguing properties of neural networks. In *International Conference on Learning Representations*, 2014. 1
- [24] Yisen Wang, Difan Zou, Jinfeng Yi, James Bailey, Xingjun Ma, and Quanquan Gu. Improving adversarial robustness requires revisiting misclassified examples. In *International Conference on Learning Representations*, 2019. 2, 3, 5, 6
- [25] Dongxian Wu, Shu-Tao Xia, and Yisen Wang. Adversarial weight perturbation helps robust generalization. *Advances in Neural Information Processing Systems*, 33:2958–2969, 2020. 3
- [26] Cihang Xie, Jianyu Wang, Zhishuai Zhang, Yuyin Zhou, Lingxi Xie, and Alan Yuille. Adversarial examples for semantic segmentation and object detection. In *IEEE International Conference on Computer Vision*, pages 1369–1378, 2017. 1
- [27] Chaojian Yu, Bo Han, Li Shen, Jun Yu, Chen Gong, Mingming Gong, and Tongliang Liu. Understanding robust overfitting of adversarial training and beyond. In *International Conference on Machine Learning*, pages 25595–25610, 2022. 2, 3
- [28] Sergey Zagoruyko and Nikos Komodakis. Wide residual networks. In *Proceedings of the British Machine Vision Conference*, 2016. 6
- [29] Hongyang Zhang, Yaodong Yu, Jiantao Jiao, Eric Xing, Laurent El Ghaoui, and Michael Jordan. Theoretically principled trade-off between robustness and accuracy. In *Proceedings of the 36th International Conference on Machine Learning*, pages 7472–7482, 2019. 2, 3, 4, 5, 6
- [30] Jingfeng Zhang, Xilie Xu, Bo Han, Gang Niu, Lizhen Cui, Masashi Sugiyama, and Mohan Kankanhalli. Attacks which do not kill training make adversarial learning stronger. In *Proceedings of the 36th International Conference on Machine Learning*, pages 11278–11287, 2020. 3
- [31] Jingfeng Zhang, Jianing Zhu, Gang Niu, Bo Han, Masashi Sugiyama, and Mohan Kankanhalli. Geometry-aware instance-reweighted adversarial training. In *International Conference on Learning Representations*, 2020. 3, 5, 6